Predicting the ultimate potential of natural gas SOFC power cycles with CO_2 capture – Part A: Methodology and reference cases

Stefano Campanari [a, *, 1], Luca Mastropasqua [a, 1], Matteo Gazzani [b], Paolo Chiesa [a, 1], Matteo C. Romano [a, 1]

[a] *Politecnico di Milano, Department of Energy, Via Lambruschini 4, 20156, Milano, Italy*
[b] *ETHZ – Institute of Process Engineering, Sonneggstrasse 3, 8092, Zurich, Switzerland*

Driven by the search for the highest theoretical efficiency, in the latest years several studies investigated the integration of high temperature fuel cells in natural gas fired power plants, where fuel cells are integrated with simple or modified Brayton cycles and/or with additional bottoming cycles, and CO_2 can be separated via chemical or physical separation, oxy-combustion and cryogenic methods. Focusing on Solid Oxide Fuel Cells (SOFC) and following a comprehensive review and analysis of possible plant configurations, this work investigates their theoretical potential efficiency and proposes two ultra-high efficiency plant configurations based on advanced intermediate-temperature SOFCs integrated with a steam turbine or gas turbine cycle. The SOFC works at atmospheric or pressurized conditions and the resulting power plant exceeds 78% LHV efficiency without CO_2 capture (as discussed in part A of the work) and 70% LHV efficiency with substantial CO_2 capture (part B). The power plants are simulated at the 100 MW scale with a complete set of realistic assumptions about fuel cell (FC) performance, plant components and auxiliaries, presenting detailed energy and material balances together with a second law analysis.

Keywords:
SOFC power cycle
Hybrid cycle
Natural gas
CO_2 capture
High efficiency

1. Introduction

In recent years, the need to limit the anthropogenic CO_2 emissions and to meet the 2 °C temperature increase scenario [1] has prompted the research to develop alternative routes for electricity production. Notably, the increase of generation efficiency and the deployment of carbon capture and storage (CCS) have been recognized as key players to fulfil this ambitious goal. Among the investigated solutions, fuel cells share the unique capability of bridging high efficiency with the possibility of capturing the produced CO_2, as anticipated since the work of Hirschenhofer et al. [2]. Additionally, thanks to their modular nature, fuel cells can be deployed in both large, centralized, and in small, decentralized, power generation units (in the order of 10–100 MW_e and 1–1000 kW_e, respectively) [3,4]. Alongside the investigation of long-term solutions, as direct [5,6] or indirect [7–13] coal-based plants, mostly centered on the concept of Integrated Gasification FC cycles (IGFC) with CCS [10–13], part of research on power production from fuel cells with and without CO_2 capture focuses on the use of natural gas (NG) as fuel. The development of NG-based fuel cell power cycles has long been investigated, mainly driven by the very high theoretical efficiency [3,14–16] and by the widespread

* Corresponding author.
E-mail address: stefano.campanari@polimi.it (S. Campanari).
[1] www.gecos.polimi.it.

Published Journal Article available at: http://dx.doi.org/10.1016/j.jpowsour.2016.05.104

Nomenclature

Ex	exergy, [MJ kg^{-1}]
FC	fuel cell
GT	gas turbine
HHV	higher heating value, [MJ kg^{-1}]
HT	high temperature
HTS	high temperature shift
HRSG	heat recovery steam generator
ICR	intercooled regenerative
LHV	lower heating value, [MJ kg^{-1}]
LT	low temperature
m	mass flow rate, [kg s^{-1}]
NG	natural gas
ORC	organic Rankine cycle
P	power, [MW]
p	total pressure, [bar]
Q	mole flow rate, [kg s^{-1}]
S	entropy, [kW K^{-1}]
SOFC	solid oxide fuel cell
ST	steam turbine
T	temperature, [°C] or [K]
U_a	air utilization factor: $U_a = O_{2,consumed}/O_{2,inlet}$
U_f	Fuel utilization factor
V	fuel cell potential, [V]
WGS	water gas shift

Subscripts

a	air
amb	ambient
el	electric
in	inlet
f	fuel
th	thermal

availability of this clean fuel. The majority of the proposed solutions aim at maximizing the plant efficiency by matching the heat bal-ance of the natural gas conversion route with the fuel cell. There-fore, they rely on high temperature fuel cells, namely Solid Oxide Fuel Cells (SOFC) and Molten Carbonate Fuel Cells (MCFC). Addi-tionally, both SOFC and MCFC feature the most reasonable possi-bilities of being industrialized up to full commercialization in the very next decades. Remarkable R&D results have been achieved during the last 10–15 years, with rather successful experimentations in terms of performance, availability and increasingly low performance degradation for both fuel cell technologies. On one hand, MCFCs have already reached a significant experience in terms of large scale installations (above 200 MW [4]) with over 50% electrical efficiency in multi-MW plants with ORC bottoming cycle and increasingly longer cell life [17]; while in the latest years SOFCs have demonstrated the potential to reach 60% + LHV electrical efficiency from natural gas even at a few kW scale [18–22]. Moreover SOFCs are increasingly applied to electric power generation, with more than 150 MW of cumulative power [23,24], showing an impressive potential for setting up future ultra-high efficiency power plants.

Based on this background, several studies have been performed in recent years on the integration of power production and CO_2 capture within NG-based SOFC, starting with early works in the nineties and around 2000 [2,25–27]. The majority of these studies consider hybrid cycles, where high temperature fuel cells are integrated with a simple or modified Brayton cycle, in some cases adding a bottoming cycle (e.g. based on steam or ORC). Despite the number of publications available in literature on this topic (see for instance the review in Ref. [28] or [29–32]), it is very difficult to fairly evaluate and compare the several plant solutions proposed, mainly because of the different methodologies and assumptions adopted. Moreover, FC performance has considerably evolved in the latest years, calling for a revision of the studies about their potential application. Accordingly, this two-part paper aims at providing an overall picture of the ultimate performance of NG-fuelled, SOFC-based power cycles with and without CO_2 capture by predicting and comparing the results on the ground of consistent assumptions and common methodology. To reach this goal, this part A paper is focused on the methodology and on the analysis of the reference configurations without CO_2 capture. Firstly, the different strategies for CO_2 capture from SOFC power cycles are discussed. Secondly, the simulation tools are explained and the SOFC technology level is defined by calibrating the results of our tool with one of recent state-of-the-art SOFC units, representative of 60% + efficient SOFCs. Finally, two different hybrid cycles without CO_2 capture are simulated by coupling the SOFC with (i) a conventional steam-based Rankine cycle, where the SOFC works at ambient pressure (SOFC + ST), and (ii) a Brayton cycle, where the SOFC is pressurized (SOFC + GT). The presented analysis is strengthened by combining considerations from both first and second law efficiency perspective. The Part B paper discusses the SOFC-based applications with CO_2 capture and compares the results with the reference cycles in terms of first and second law efficiency; moreover, it carries out a sensitivity analysis of the results towards the most important SOFC performance parameters.

2. SOFC power cycles

2.1. SOFC technology

Solid oxide fuel cells are nowadays considered among the most promising fuel-to-electricity conversion units, at least when the primary fuel is a hydrocarbon like natural gas. Indeed, as shown in Fig. 1, they are able to outperform competitive power technologies in most of the power range of interest. When coupled with gas turbine or other thermodynamic cycles in 'hybrid' configurations, they are expected to reach 70% + class electric efficiencies, which make them suitable for ultra-high efficiency power generation from natural gas.

Focusing on the case of natural gas feeding, the process occurring in the SOFC (see Fig. 2) consists in the conversion of hydrocarbons to a H_2 and CO mixture through reforming reactions and the oxidation of the fuel in the anode with oxygen ions extracted from the air at the cathode side and transported across an oxygen ion-conducting ceramic electrolyte (classically based on Yttria-stabilized ZrO_2, or doped Cerium oxides for the lower tempera-ture range). Besides the intrinsic efficiency gain induced by the electrochemical oxidation, the spent fuel and the exhaust gases are not mixed with the depleted air, which makes the gas composition particularly suitable for an efficient CO_2 removal process. Additionally, as discussed in Section 2.2, one of the key advantages of high temperature fuel cells is the possibility to internally sustain the natural gas reforming process, exploiting the fuel cell exhaust heat to drive the endothermic reforming reactions.

First SOFC installations at around 100 kW scale were

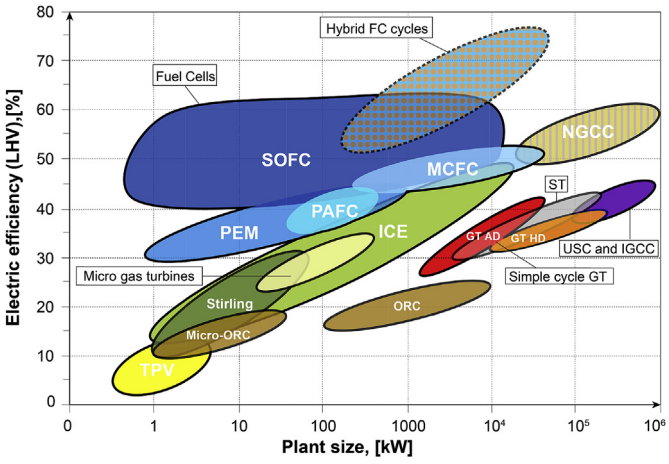

Fig. 1. General schematization of the attainable electrical efficiency as a function of plant size in state-of-the-art, fuel-based, power generation solutions (with special attention on the use of natural gas). The area of Hybrid FC cycles reports an expected (calculated) efficiency range for FC cycles with gas and/or steam turbines.(PEM = polymeric electrolyte fuel cell; PAFC = phosphoric acid fuel cells; MCFC = molten carbonate fuel cells; SOFC = solid oxide fuel cell; ORC = Organic Rankine Cycle; ICE = internal combustion engines; TPV = thermo-photovoltaic units; GT AD/HD = aero-derivative or heavy duty gas turbines; ST = conventional steam turbine cycles; USC = ultra super-critical steam cycles; NGCC = natural gas combined cycles; IGCC = integrated gasification combined cycles). (Adapted from Ref. [33]).

demonstrated by Siemens-Westinghouse in the '90s based on 1000°C-class tubular solid oxide fuel cells [3,14]; few years later, small scale hybrid systems with recuperated gas turbine cycles were tested demonstrating 55% efficiency, with projected performance up to 65–70% [14,34,35]. However, in the last decade R&D activity on SOFCs has been concentrated on lowering the fuel cell operating temperatures, due to concerns about manufacturing costs, high temperature materials and cell reliability issues which have proven to be extremely challenging at the original operating temperatures. Nowadays, most SOFC manufacturers are concentrating their efforts around "Intermediate Temperature" SOFC (IT-SOFC), i.e. 700–800 °C [4,20,23,36], or even around lower temperature, i.e. 500–600 °C, based on updated material formulations and manufacturing processes [37]. Keeping the advantages of an integrated natural gas reforming process, they have considerably improved performance in terms of power density, efficiency and resistance to thermal cycles, increasing their chances for a successful industrialization [4,38].

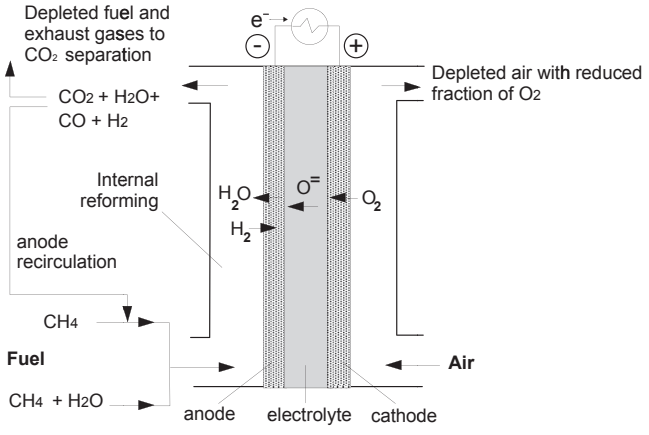

Fig. 2. Operating principles of a SOFC.

2.2. Configurations of SOFC power cycles with and without CO_2 capture

A large number of possible plant configurations is proposed in the open literature for large scale SOFC-based power plants. An overview of the possible strategies for integrating a solid oxide fuel cell in a fossil-fuel power cycle without and with CO_2 capture is represented in Fig. 3, based on an adaptation of the diagram proposed by Ref. [28]. Each node in the figure represents an alternative option, which combined can lead to a wide variety of possible configurations.

Focusing on the case of natural gas and depending on the type of FC integration with the fuel preparation or processing, two main plant solutions can be identified: (i) systems where natural gas is – partially or totally – internally reformed in the fuel cell [26,30,39,40] and (ii) systems where natural gas is reformed before the fuel cell, which is therefore fed with a hydrogen rich syngas [29,41]. Since steam reforming is an endothermic reaction (see eq. (1)), heat must be supplied to drive the reforming process. The reaction energy can be recovered from the fuel cell itself or taken from an external source (e.g. burning part of the fuel), which adds an energy consumption and reduces the efficiency. In the first option the reaction is carried out "internally" or in close thermal integration with the fuel cell stack [25,26,34,42], where most of the reforming reactions (see Eq. (1)) are developed. In this way, the fuel cell waste heat is usefully turned into chemical energy of the reformed fuel stream and hence reused in the fuel cell increasing its efficiency for a given fuel utilization factor. In addition, the heat taken by steam reforming reaction reduces the air flow rate needed for fuel cell cooling, hence reducing the flue gas flow rate at the plant stack and the associated heat losses, further contributing to improving the overall system efficiency.

$$C_xH_y + xH_2O \leftrightarrow (y/2 + x)H_2 + xCO$$

$$\begin{aligned} &CH_4: \Delta H^{\circ}_r = +206.2\ \text{kJ mol}^{-1} \\ &C_2H_6: \Delta H^{\circ}_r = +347.3\ \text{kJ mol}^{-1} \\ &C_3H_8: \Delta H^{\circ}_r = +497.7\ \text{kJ mol}^{-1} \end{aligned} \quad (1)$$

This thermal integration could be in principle obtained by transporting heat from the fuel cell to an external reformer [29], for instance introducing a heat transfer loop. However, this approach makes the plant more complex, requiring to add high temperature heat exchangers, and introduces heat and parasitic losses due to hot fluid circulation. A recent analysis has shown how this affects the expected performance, significantly decreasing the efficiency with respect to theoretical estimations [31].

Accordingly, most of the proposed solutions rely on the thermal integration between fuel cells and natural gas reforming/shift section, either with dedicated stack layers (also known as Indirect Internal Reforming, IIR) or with a direct integration at the fuel cell anode (Direct Internal Reforming, DIR) [3,43], improving also the system compactness. Internal reforming requires a careful management of the internal temperature profile, which typically shows a steep change at anode inlet due to the fast reforming kinetics [44,45]. With the aim of limiting the thermal gradients and the stack stresses, an adiabatic pre-reforming reactor is generally added before the SOFC anode inlet, converting part of the hydrocarbons (and specifically cracking the higher hydrocarbons) before the fuel cell. This solution also allows reducing the risk of carbon deposition within the fuel cell stack. Some researchers proposed to extend the concept to a complete adiabatic external reforming [42], showing high overall efficiency but requiring substantial fuel recirculation with blowers to transfer sensible heat to the reactor and to allow completing the reforming reactions.

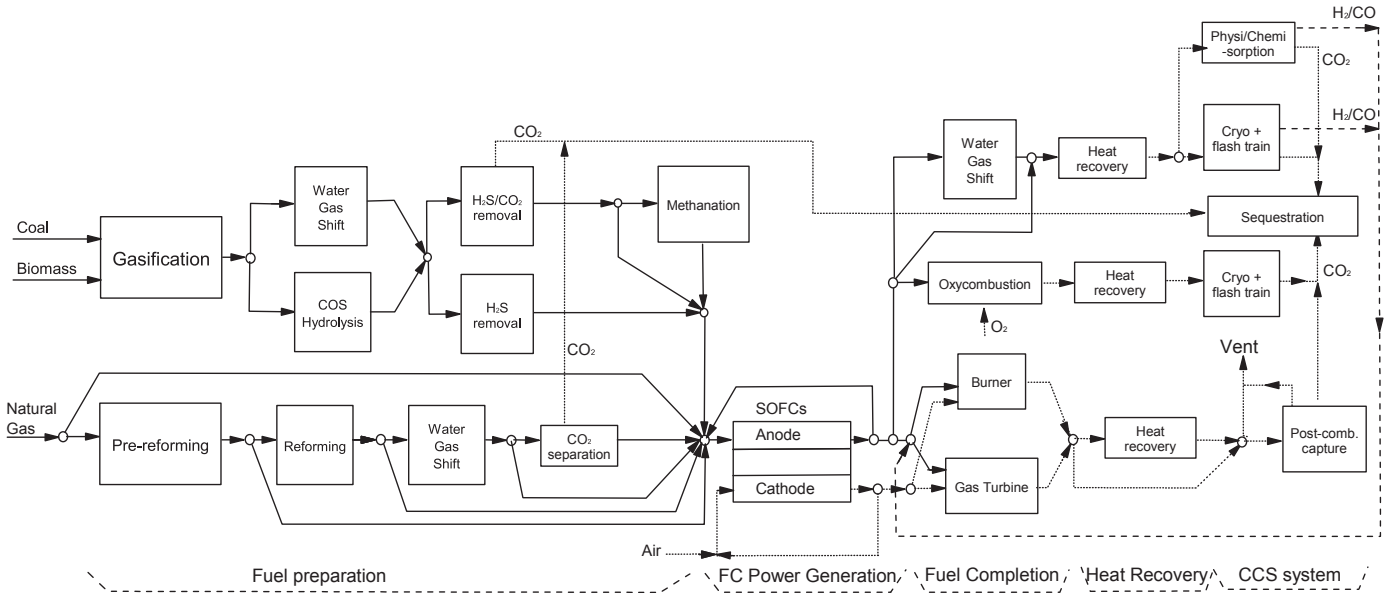

Fig. 3. Overview of conceptual strategies and alternatives for integrating a solid oxide fuel cell in a fossil-fuel power cycle with CO_2 capture (adapted from Ref. [28]).

Steam required for NG reforming (both internal and external reforming) can be fed from an external water source (e.g. recovering condensed water and raising steam through heat recovery from system exhaust gases) [30] or obtained by recycling part of the anode exhaust stream [26]. This second solution also enhances the global fuel utilization across the fuel cell for a given single passage fuel utilization, which can be relatively low since part of the un-converted fuel at the anode outlet is recycled to the SOFC inlet. Anode recycle can be obtained by a blower or by an ejector driven by higher pressure fuel [47]. Despite the rather low thermodynamic efficiency of the ejector-based compression process, this may be preferable in case high pressure fuel is available as it would allow a high temperature recycle while avoiding the blower electric consumption.

An additional WGS reactor can be added before the fuel cell, which however increases the plant cost and complexity. This option is proposed in literature only for pre-SOFC CO_2 capture configura-tions, where a H_2-based fuel is fed to the fuel cell [41,46,48].

In case a solid feedstock as coal or biomass is used, fuel is first converted to syngas, then cleaned and finally fed to the SOFC. The syngas sweetening consists in a desulphurization process, since the content of sulphur species (H_2S and COS) in syngas derived from solid feedstock gasification is much higher than in natural gas. Nevertheless, desulphurization is applied also to natural gas in order to cope with the low levels (<0.1 ppm) required by SOFCs [3,49]. Similarly to the natural gas case, pre-SOFC WGS and CO_2 separation can be employed. Alternatively, a partial CO_2 removal and a following methanation stage can be envisaged in order to enrich the syngas with methane and take advantage of the benefits deriving from internal reforming [50].

Another degree of freedom in the design of a SOFC system is air preheating. In order to avoid excessive thermal stresses through the fuel cell, gas temperature increase along the stack should be limited. To this end, heat can be recovered from the gases leaving the fuel cell (or the combustor if adopted) by means of high temperature heat exchangers (600–800 °C) [26,30,51] or by recycling and mixing part of the cathode exhaust with fresh air [52,53]. While the first option implies the use of expensive material, the second requires the adoption of an ejector to sustain the recycle, thus increasing the auxiliary electric consumptions (fresh air needs to be pressurized to serve as primary driving gas in the ejector). As the two options affect primarily the CAPEX and the OPEX respectively, the choice is driven by an economic analysis.

A major impact on the plant configuration and performance is associated to SOFC operating pressure. Pressurized SOFC entails the operations in hybrid configuration with a gas turbine cycle. Both configurations with moderate pressure (3–6 bar) [26,30] and high pressure (around 20–30 bar) [15,51] SOFCs have been proposed. In the first case, current SOFC technology can be adopted, usually in combination with gas turbines with moderate turbine inlet temperatures (up to 900–950 °C), not requiring blade cooling. In the second case, which is indicated for longer term applications, pressurized planar SOFC should be coupled with low firing temperature gas turbine engines [54], preferably of large size to take advantage of the higher turbomachinery efficiency. In this case, a bottoming heat recovery steam cycle is also adopted, so that the combination of a topping SOFC with a high efficiency bottoming combined cycle (gas turbine + steam cycle) can lead to high plant efficiencies. However, most of the SOFCs proposed by manufacturers operate at atmospheric pressure. On one hand, this leads to lower plant costs, since stacks can be enclosed in atmospheric pressure vessels. On the other hand, pressurization would contribute in increasing SOFC voltage and efficiency, thanks to the higher partial pressure of the reactants.

When configurations with CO_2 capture are considered, a number of additional process variables has to be defined. A first option is to adopt a pre-anode CO_2 capture configuration, entailing a fuel treatment section based on steam reforming and water gas shift to produce a H_2/CO_2-based syngas. CO_2 and H_2 can then be separated by conventional gas separation processes (e.g. by absorption, adsorption, membranes) thus resulting in a fuel cell fed with a H_2-rich fuel [29,30].

Alternative options involve post-anode CO_2 capture, aiming at removing the CO_2 after the partial fuel oxidation in the SOFC. Such configurations may take advantage of the air separation intrinsically performed by the SOFC, which produces anode exhaust gases equivalent to the product of partial oxidation by pure oxygen. One option for post-anode CO_2 separation is therefore to complete oxidation with high purity oxygen by oxy-fuel combustion [25,26,55]. This process produces a stream of H_2O and CO_2, from

which high purity CO_2 can be obtained after water condensation. While making CO_2 separation simple, pure O_2 production by conventional cryogenic processes is highly energy-demanding and suffers strong scale effects, so that this system becomes most competitive for very large plant sizes [56]. A second option for post-anode CO_2 separation is to treat the anode exhaust in a WGS reactor, converting the residual CO into CO_2 and H_2. CO_2 can then be separated and the H_2 stream may be partly recycled to the fuel cell inlet or burned, for example with the cathode exhaust stream. Among the possible CO_2 separation processes (e.g.: PSA [57], membranes [58]), low temperature CO_2 condensation appears particularly attractive [59], since CO_2 concentration after the post-anode WGS reactor is high (the higher the fuel utilization factor, the higher the final CO_2 concentration) and no solvent or other chemical processes are needed. A competitive option to low temperature phase change separation is physical absorption [25,26]. The last post-anode option for CO_2 capture is chemical absorption on the flue gases resulting from SOFC exhaust combustion [25,30]. While this option would be based on the most consolidated separation process, it would operate with the lowest CO_2 partial pressure stream available and would lose the intrinsic advantages introduced by the SOFC in acting as a partial oxidation reactor with pure oxygen.

The relations among all the different process configuration options discussed above, as well as their main advantages and disadvantages, are summarized in Table 1.

2.3. Maximum theoretical efficiency

Before assessing the potential of high-efficiency power cycles generating electricity from natural gas with CO_2 capture, it is interesting to define the theoretical efficiency limit which could in principle be achieved by such cycles.

For an ideal mixture of ideal gases, the maximum work which can be generated by a series of reversible processes taking a mass unit of the mixture from its current condition (assigned as pressure and temperature, respectively p and T) to thermodynamic equilibrium with a reference environment (at p_0, T_0) is equal to its exergy, according to the expression [60]:

$$Ex = (h - h_0) - T_0(s - s_0) + RT_0 \sum x_i \ln \frac{x_i}{x_{i,0}} \quad (2)$$

Where, x_i and $x_{i,0}$ are the molar fraction of the i-th chemical species considered in the given mixture and in the reference environment.

The exergy of a fuel can be inferred by applying Equation (2) to a mass unit of fuel reacting in proportion with α kg of oxidizer while producing $(1 + \alpha)$ kg of products. In the assumption that fuel and oxidizer are at the reference conditions, the following expression can be applied:

$$Ex_{f,0} = \left[h_{f,0} + \alpha \cdot h_{O,0} - (1+\alpha)\cdot h_{p,0}\right] - T_0\left[s_{f,0} + \alpha \cdot s_{O,0} - (1+\alpha)\cdot s_{p,0}\right] + RT_0 \sum x_{i,p} \ln \frac{x_{i,p}}{x_{i,0}} \quad (3)$$

If the fuel is available at conditions (p, T) different from the reference ones, the additional contribution given by the first two terms of Equation (2) has to be accounted for:

$$Ex_f = Ex_{f,0} + \left(h_f - h_{f,0}\right) - T_0\left(s_f - s_{f,0}\right) \quad (4)$$

Considering the case of the assigned natural gas available at 20 bar and 15 °C, the resulting fuel exergy is 48.193 MJ kg^{-1}.

When CO_2 capture and storage are performed, in order to fairly account for the maximum work of the fuel, the previous exergy figure has to be corrected for the energy required by the CO_2 separation and compression process. This term equals the exergy of CO_2 at T_0 and pressure leaving the plant.

$$Ex_{CO2} = (h_{CO2} - h_{CO2,0}) - T_0(s_{CO2} - s_{CO2,0}) + RT_0 \ln \frac{1}{x_{CO2,0}} \quad (5)$$

Where, $x_{CO2,0}$ is the concentration of CO_2 in the environment (400 ppm). When the properties of the CO_2 are calculated according to [61], the exergy of CO_2 at p = 150 bar and T = 15 °C calculated from expression (4) is equal to 632.7 kJ $kg^{-1}$of CO_2. Since the combustion of 1 kg of natural gas releases 2.649 kg of CO_2, the corrected fuel exergy is 46.517 MJ kg^{-1}

In terms of net efficiency, the maximum theoretical value achievable by reversibly exploiting the fuel in a plant with CO_2 capture is 100.08% and 90.41% when the fuel LHV and HHV are respectively assumed as reference.

3. Simulation tools and SOFC performance

3.1. Simulation tools

The thermodynamic modelling of the assessed power cycles is carried out with the modular simulation code "*GS*", a tool that has been developed since early 90's at the Energy Department of Politecnico di Milano [62]. It can provide highly accurate results in a variety of complex plant configurations, including gas turbine cycles, combined cycles [63], coal based power plants [64] and hybrid cycles [15,65]. The code integrates models for the prediction of gas and steam turbines and FC performance [30,35] and has been applied to benchmark CO_2 capture power plants within specific EU projects [66].

The plant scheme is reproduced by assembling in a coherent network the different components selected in a library containing over 20 basic modules. Built-in rules allow predicting turbomachines (gas and steam turbines, compressors) efficiency as a function of their operating conditions and size. The SOFCs can be modelled through a lumped volume or zero-D approach, which calculates mass and energy balances (for more specific investigations, 2D finite volume codes, able to delve into voltage prediction, current density and temperature distribution profiles, are also developed to run in connection to GS). The model requires to assign the reactant properties at FC inlet (temperature, pressure, chemical composition and mass flow rate at anode and cathode inlet), the fuel utilization factor (U_f) inside the fuel cell and the cell voltage (V_c); then it calculates the outlet stream compositions, temperatures and electrical output in order to close the overall energy balance of the fuel cell. According to the simulation requirements it can also run iteratively to set inlet/outlet temperatures and/or reactant utilization according to other boundary variables.

Coupled with the GS models, the energy balances of the CO_2 separation technology with liquefaction and compression are simulated with ASPEN Plus™ [67].

3.2. SOFC performance and simulation assumptions

In this work the SOFC is simulated assuming the performance of latest generation IT-SOFC, featuring 60%-class net electric efficiency in power generation from natural gas. Different manufacturers have reported the achievement of such high system efficiency, including Ceramic Fuel Cell Ltd (CFCL, Australia) [18,19], Fuel Cell Energy Inc. (USA) [17,20], Solid Power (Italy) [21], Bloom Energy (USA) [23,24], obtained from high efficiency stacks that are typically able to run at 65–68% DC gross efficiency. In this work, we

Table 1
Main advantages and disadvantages of different plant configuration options and mutual dependencies, for natural gas-fed plants with and without CO_2 capture.

	Option code	Option description	Relation with other options	Advantages and disadvantages
Steam reforming	A	Adiabatic pre-reforming	Excludes option B	+ Converts higher hydrocarbons and reduces the risk of carbon deposition in the fuel cell or in the downstream reformer.
	B	Heat exchange pre-reforming by waste heat recovery	Excludes options A	+ Converts higher hydrocarbons and reduces the risk of carbon deposition in the fuel cell or in the downstream reformer. + Efficient recovery of medium-high temperature heat by chemical recuperation of sensible heat + Limited temperature variations in the fuel cell thanks to the feeding of the FC with a low-CH_4 fuel, leading to a reduced SOFC internal reforming − Higher air flow rate in the FC needed to keep a target FC gas exit temperature − Higher capital cost than adiabatic pre-reforming
	C	External reforming by autothermal or fired tubular reforming	Excludes option D	+ Avoids the need of steam reforming catalyst in the FC + Minimal temperature variations in the fuel cell thanks to the minimal CH_4 content in the FC fuel. − Maximum air flow rate in the FC needed to keep a target FC gas exit temperature − Maximum capital cost for fuel processing
	D	Internal reforming SOFC	Excludes option C	+ Efficient recovery of high temperature heat generated in the FC + The higher the internal reforming, the lower the air flow rate to keep a given FC gas exit temperature thanks to the heat absorbed by reforming reaction. Lower air flow rates result in higher plant efficiency (higher combustion temperature of FC off-gases, lower stack losses) + Simpler and more compact overall configuration because it avoids external heat exchangers and reactors − Need of reforming catalyst on anode surface: higher fuel cell cost − Lower SOFC power density for given voltage, due to the kinetics of steam reforming limiting the fuel conversion process, especially in intermediate-low temperature SOFC. − Higher temperature variations in the FC due to the endothermic nature of the steam reforming reaction
SOFC fuel WGS	E	Pre-SOFC WGS	Needs option C Excludes option F	+ Risk of carbon deposition in the FC is minimized by feeding H_2 − Increases plant complexity
	F	Internal WGS SOFC	Excludes option E	+ More compact and simpler configuration
SOFC fuel humidification	G	Steam from boiler	Excludes options H, I	+ Simple and easily controllable system − Demi-water consumption, eventually emitted to the atmosphere in case of configuration with no water recovery
	H	Anode recycle by blower	Excludes options G, I	+ No additional water consumption − Additional electric consumption
	I	Anode recycle by ejector	Excludes options G, H	+ No additional water consumption + High temperature recycle possible, contributing to fuel preheating to high temperature + No additional power consumption, if primary fuel is available at sufficiently high pressure and pressure energy is not recovered by a fuel expander. − In case primary fuel is available at low pressure (or a fuel expander is used), this is a dissipative system, which requires a higher compression power (or leads to lower power generation from fuel expander) than a recycle blower.
SOFC air final preheating	J	High temperature heat exchanger	Excludes option K	+ Efficient system, recovering high temperature waste heat from the FC. − Need of high temperature and high cost heat exchanger
	K	Ejector driven cathode recycle	Excludes option J	+ Cheap and compact system, not requiring high temperature heat exchange surfaces − Dissipative system, lead to higher electric consumption for air compression
	L	Atmospheric pressure SOFC with bottoming Rankine cycle	Excludes options M, N	+ Maximum plant simplicity − Lower cell performance because of the lower

(*continued on next page*)

Table 1 (*continued*)

	Option code	Option description	Relation with other options	Advantages and disadvantages
SOFC operating pressure and bottoming cycle				Nernst potential (for the same inlet composition and temperature) compared to alternative options.
	M	Moderate pressure (4–8 bar) SOFC with low β regenerative gas turbine cycle (uncooled turbine) and optional Rankine cycle	Excludes options L, N	+ Increased SOFC performance thanks to the increased Nernst potential − Increased plant complexity due to the need of balancing air and fuel channels' pressure and of containing vessel for the FC
	N	High pressure (≈20–30 bar) SOFC with high β and high temperature gas turbine cycle (cooled turbine) and Rankine cycle	Excludes options L, M	+ Maximum plant efficiency + A relevant portion of the total power output is generated by the gas turbine cycle, which has a lower specific cost than the FC. This may have a positive effect on the overall plant Capex. − Maximum plant complexity
CO_2 capture process	O	Oxycombustion of anode exhaust	Excludes options P, Q, R	+ Relatively low O_2 consumption expected (reducing for increasing SOFC fuel utilization factors) + A virtually complete CO_2 capture efficiency is possible − High energy consumption for oxygen production − High cost of ASU, especially at small size, negatively affects overall plant Capex
	P	WGS on anode exhaust and CO_2/H_2 separation	Excludes options O, Q, R Needs options S or T	+ No need of further steam dilution, since water produced in the cell by hydrogen oxidation leads to high S/C + H_2 can be recovered and efficiently converted by partial recycle to the FC or by combustion in the bottoming cycle (especially in case of a gas turbine cycle) − CO_2 capture efficiency highly depends on the fuel utilization in the SOFC
	Q	Pre-SOFC hydrogen production and H_2/CO_2 separation	Needs options C, E, S Excludes options O, P, R	+ Simple configuration in case pre-SOFC steam reforming and WGS are selected for optimal operation of the FC − Solvent system needed for CO_2 absorption due to the relatively low CO_2 concentration − Does not exploits the intrinsic capability of N_2 free fuel oxidation of SOFCs
	R	Post-SOFC chemical absorption on air-combusted anode gas	Excludes options O, P, Q, S, T	+ No effect on the base SOFC plant without CO_2 capture: easily retrofittable − Solvent system needed for CO_2 absorption due to the low CO_2 concentration − Does not exploits the intrinsic capability of N_2 free fuel oxidation of SOFCs − Low energy efficiency expected due to the heat required for solvent regeneration
CO_2/H_2 separation process	S	Physical/chemical absorption	Needs options P or Q Excludes options O, R, T	+ Do not need high CO_2 concentrations for efficient separation + CO_2 is released at intrinsically high purity − Heat required for chemical solvent regeneration − Lower energy efficiency expected compared to low temperature phase separation, in case of high initial CO_2 concentrations
	T	Low temperature phase separation	Needs option P Excludes option O, Q, R, S	+ Efficient system in case of high initial CO_2 concentrations − Needs high fuel utilization factors

take as representative example the unit proposed by CFCL: it is a micro-CHP unit (1.5–2 kW range) rated at 60% net LHV efficiency (AC) and fed with natural gas, to the author's knowledge representing the first unit originally proposed on the market at this efficiency level. The cell has the ability to work at about 750 °C with very high air utilization factor (low excess air) and a limited steam-to-carbon ratio in the reforming process. The unit model has been calibrated against the available energy balances [18], which have been experimentally confirmed in several pilot installations [68,69].

The system layout is given in Fig. 4, reflecting the plant scheme reported in Ref. [18] for the micro-CHP system: the fuel utilization is 85% and the temperature of the air stream increases from about 740 °C to 780 °C in the fuel cell. The stack is composed of 51 cells operating at 43.7 V, resulting in an average cell voltage of about 0.86 V. The corresponding energy balances have been reproduced with the code GS, yielding the results summarized in Table 1. Inlet and outlet temperatures at the air side across the fuel cell (735 °C and 774 °C) reproduce with good accuracy the balances reported by the manufacturer. On the fuel side, it is assumed a temperature of 380 °C after the pre-reformer and 500 °C at the cell inlet; the steam-to-carbon ratio at anode inlet is assumed equal to 2.16.

The air utilization factor has been set to 30.5%, together with assuming an appropriate air dilution after the burner, in order to respect a final temperature at heat exchanger inlet (point #9 in Fig. 5) of 830 °C. The mass flow rates are calibrated to yield a gross SOFC power output of 1713 W which corresponds to a net electrical efficiency of 61.2% (LHV) starting from a thermal power input of

2452.2 kW_{th} (LHV-based), with 221 W of auxiliaries and inverter losses. Calculation are consistent with the power balance reported in Ref. [18], where the efficiency is 61.3% at the same gross and net power output.

integration for the connection of a large network of FC stacks with a centralized gas turbine system, as proposed in this work. System design would therefore bring about layout-specific losses (e.g. piping thermal and pressure losses) which are not considered in

Table 2
Flow properties and composition (% mol.) in the most relevant points of the SOFC module with the layout of Fig. 4.

Stream	T [°C]	P [bar]	G [mol s^{-1}]	M [kg s^{-1}]	Composition [%mol]								
					Ar	CH_4	C+	CO	CO_2	H_2	H_2O	N_2	O_2
1	15.0	1.2	3.08E-03	5.30E-05	–	91.2	4.5	–	–	–	–	4.3	–
2	350.0	1.2	1.01E-02	1.74E-04	–	29.2	–	1.4	–	2.9	65.1	1.3	–
3	20.0	1.2	8.35E-02	2.41E-03	0.9	–	–	–	0.0	–	1.0	77.3	20.7
4	500.0	1.1	1.01E-02	1.74E-04	–	29.2	–	1.4	–	2.9	65.1	1.3	–
5	735.0	1.1	8.35E-02	2.41E-03	0.9	–	–	–	0.0	–	1.0	77.3	20.7
6	771.9	1.1	1.60E-02	3.40E-04	–	–	–	2.0	17.3	9.5	70.4	0.8	–
7	771.9	1.1	7.83E-02	2.24E-03	1.0	–	–	–	0.0	–	1.1	82.4	15.5
8	911.6	1.1	9.33E-02	2.58E-03	0.8	–	–	–	3.3	–	14.6	69.3	12.0
9	830.0	1.0	1.04E-01	2.89E-03	0.8	–	–	–	3.0	–	13.2	70.1	12.9
10	125.6	1.0	1.04E-01	2.89E-03	0.8	–	–	–	3.0	–	13.2	70.1	12.9
11	15.0	1.2	6.72E-03	1.21E-04	–	–	–	–	–	–	100	–	–
12	615.7	1.2	6.72E-03	1.21E-04	–	–	–	–	–	–	100	–	–
13	20.0	1.2	1.08E-02	3.10E-04	0.9	–	–	–	0.0	–	1.0	77.3	20.7

Comparably similar performance and operating conditions are reported also for other 60%-class efficient SOFCs, although they may have different plant arrangements. As an example, the authors recently applied the same modelling approach to other types of SOFCs, according to available literature details, confirming the validity of these results [22].

The same kind of fuel cell – keeping the same reformer arrangement, overall fuel utilization factor and voltage – has been used to simulate the performance of a large scale power plant with and without CO_2 capture, as discussed in the following Section. The idea of keeping the same FC operating features when running on a much larger scale must not surprise, since fuel cells are inherently a highly modular technology. However, on a larger scale some advantages would appear in terms of improved auxiliary system efficiency due to scale effects (e.g. blowers and fans, DC/AC conversion losses). On the other hand, some difficulties may arise from the necessity of redesigning the system the simulations. Losses are in fact calculated as concentrated on each main component (heat exchangers, splitters and mixers, chemical reactors); it is worth noting that the proposed plant configurations take into account the necessity of limiting the maximum piping temperatures and pressures to reasonable values throughout the cases assessed.

The design point calculation assumptions of the SOFC-based power plants, which will be described in Section 4, are reported in Table 3.

4. Reference power cycles

This section describes the two natural gas fed SOFC-based power plants, taken as a reference in this work. In both cases, the fuel power input has been fixed to 100 MW_{th} (based on natural gas LHV). The first configuration discussed (Section 4.1) exploits the integration of an atmospehric SOFC with a steam cycle, whilst the

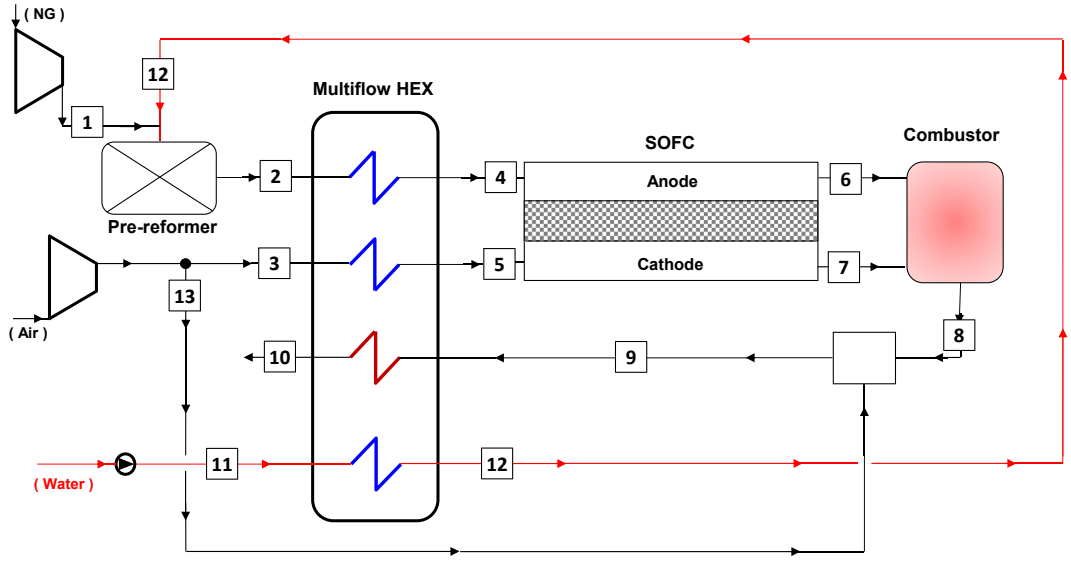

Fig. 4. Layout of the IT-SOFC module calibrated against the performance of the SOFC unit assumed as a reference. Mass and energy balances are reported in Table 2.

second one features a pressurized SOFC with an ICR gas turbine engine (Section 4.2).

It is worth nothing that in both cases steam required for NG reforming is supplied by recirculating part of the anodic product through an ejector rather than generating steam in a dedicated heat exchanger. Although this plant modification departs from the SOFC configuration described in Section 3.2, the cell anodic recycle is a well-known solution (applied in the past [14,52] as well as today by several of the quoted manufacturers) which eliminates the need of steam pipeline and heat exchanger sys-tem, taking steam from the oxidized products to sustain the reforming process. This arrangement avoids additional water consumption and the costs associated to water treatment; an issue of utmost importance for medium/large scale applications as those studied in this work. The adoption of anode recirculation brings about another key difference with respect to the config-uration in Section 3.2, since the same overall fuel utilization (kept at 85%) is now reached with a much lower single-pass fuel utilization, set at 67.2%. Reducing the single-pass fuel utilization allows decreasing the cell temperature, current density and reactant composition gradients. In addition, recent studies report a general rise of the fuel cell performance [71,72] along with the ability of the pre-reforming reactor to reach chemical equilib-rium [42] when the anode off-gas recirculation is adopted, compared to that without anodic recycle. The recycle mass flow is determined in order to ensure a steam-to-carbon ratio (S/C) at the pre-reformer inlet of 2.0, coherently with the reference case of Fig. 2. The pre-reforming reactor works adiabatically and is calculated at equilibrium.

4.1. Atmospheric pressure SOFC + ST cycle

As already mentioned, the first reference power cycle is based on the integration of an ambient pressure operating SOFC with a steam turbine (ST) bottoming cycle (Fig. 5). SOFCs are arranged in a network of modules, each including a high temperature air pre-heater, a burner for anode off-gas combustion and an anode recycle loop based on ejectors, driven by the primary NG feeding.

Prior entering the SOFC module, the natural gas pre-treatment section consists of a low temperature desulphurization reactor. Sulphur compounds in natural gas are related to traces of H_2S as well as to odorants (mercaptans, tiophenes). Desulphurization is carried out to respect the tolerance limit of SOFC catalytic materials, generally Ni-based, which require to work below 0.1 ppm of total sulphur content [3]. The desulphurization reactor is a commercially available technology [49] and consists of a fixed bed, temperature swing-based, adsorption process. Natural gas is desulphurised flowing at ambient temperature through the sulphur-selective adsorbent. When the sulphur compound front reaches the end of the bed, natural gas is switched to a different column while the spent bed undergoes the temperature-based regeneration process. Sorbent is typically regenerated at 300 °C by flowing a purge stream (e.g. air, nitrogen).

Afterwards, the desulphurised natural gas mixes with the anodic recycled stream throughout the use of an ejector; the required recycle rate to ensure an S/C = 2 is approximately 64% of the total anode outlet stream.

The fuel cell configuration is assumed to reproduce on a larger scale the performance discussed in Section 3.2. In order to respect the reference operating conditions, a once-through (i.e. between point #15 and #16 in Fig. 6) fuel utilization factor has been set to approximately 67.2%, in order to obtain the expected global U_f value (85%) (i.e. between point #13 and #17). It is worth noting that, original cells may have specific flow field arrangements and multiple-pass flow designs exploited to reach the declared U_f; despite these geometrical configurations are not considered in the present modelling, the adopted assumptions permit to comply with overall cell balances and global U_f , which are therefore correctly reproduced. The inlet and outlet temperatures of the cell stack have been slightly modified with respect to the reference case in order to meet the additional plant assumptions and constraints.

At the outlet of each SOFC stack, an off-gas combustor is employed to complete the oxidation of the non-recycled stream leaving the anode. The combustion exploits the oxygen remain-ing in the fuel cell cathode outlet stream, which is sufficient to respect the assumed limit of the minimum oxygen fraction at combustor outlet of 1.5%. In order to meet the constraints on the minimum O_2 molar fraction at the combustor outlet, it was necessary to toggle the air inlet temperature, with respect to the reference case previously introduced. The temperature level at the cell inlet indeed influences the air flow rate required to cool the cell, which depends on the imposed fuel utilization factor. Consequently, a change in the inlet temperature leads to a change in the air mass flow rate and therefore of the O_2 molar fraction.

All these components lie within the boundaries of the 'SOFC module' evidenced by the dashed line in Fig. 5, representing the repeated unit that builds up the FC network. In addition, each SOFC module includes a cathodic air pre-heater, which operates using the hot gases exiting the combustor (point #6) to preheat inlet air (from point #3 to point #4); the preheater (which is represented for simplicity as a single unit) includes a counter-flow and a co-flow section, in order to decrease the maximum wall temperatures at the hot end, as shown in the lower part of Fig. 5. This set of modular heat exchangers located within the 'SOFC module' is employed mainly to reduce the temperature of the external pipeline network which supplies the spent fuel to the centralized steam bottoming cycle, allowing the use of less expensive materials and reducing heat losses. The same modular arrangement will be adopted later for the pressurized configuration, which relies on a centralized gas turbine cycle.

Hot gases exiting the modules at around 650 °C (point #7) are transported to a centralized steam cycle, producing high pressure superheated steam (T = 400 °C, p = 40 bar) in a heat recovery boiler, as evidenced by the temperature-heat duty diagram in the lower part of Fig. 5.

The SOFC air utilization factor has been considered to attain a cell outlet temperature of 800 °C, according to the value pro-posed by the manufacturer [18]; the final air utilization factor is 78.3%. The remarkably higher air utilization, with respect to the reference case of Fig. 5 (where $U_{air} = 30.5\%$), reflects (i) a moderately higher temperature rise of the air stream (46 °C vs. 35 °C at the cathode), however well below critical values; and
(ii) a different mass flow rate proportion of the reactant streams entering the fuel cell: while in the first case the great majority of heat generated by the cell was transferred to the cathode stream, here the adoption of anode recycle brings about a higher (in relative terms) anode flow rate (stream #15), featuring a higher heat capacity, so that heat is transferred with a more equilibrated ratio to the cathode and anode streams. The resulting specific work of the fuel cell is 1866 kJ kg_{air}^{-1} and 3919 kJ kg_{fuel}^{-1} vs. 710.8 kJ kg_{air}^{-1} and 9844 kJ kg_{fuel}^{-1} of the first calibration case. On the other hand, we neglect any effect of the variation of air utilization on the cell voltage, which is kept at the same value of the first calibration (0.86 V); the minimum oxygen content at the cathode outlet (stream #5) is anyway above the assumed limit of 5%.

It is worth noting that the achievement of high voltages with high reactant utilization, as proposed in this simulation, calls for

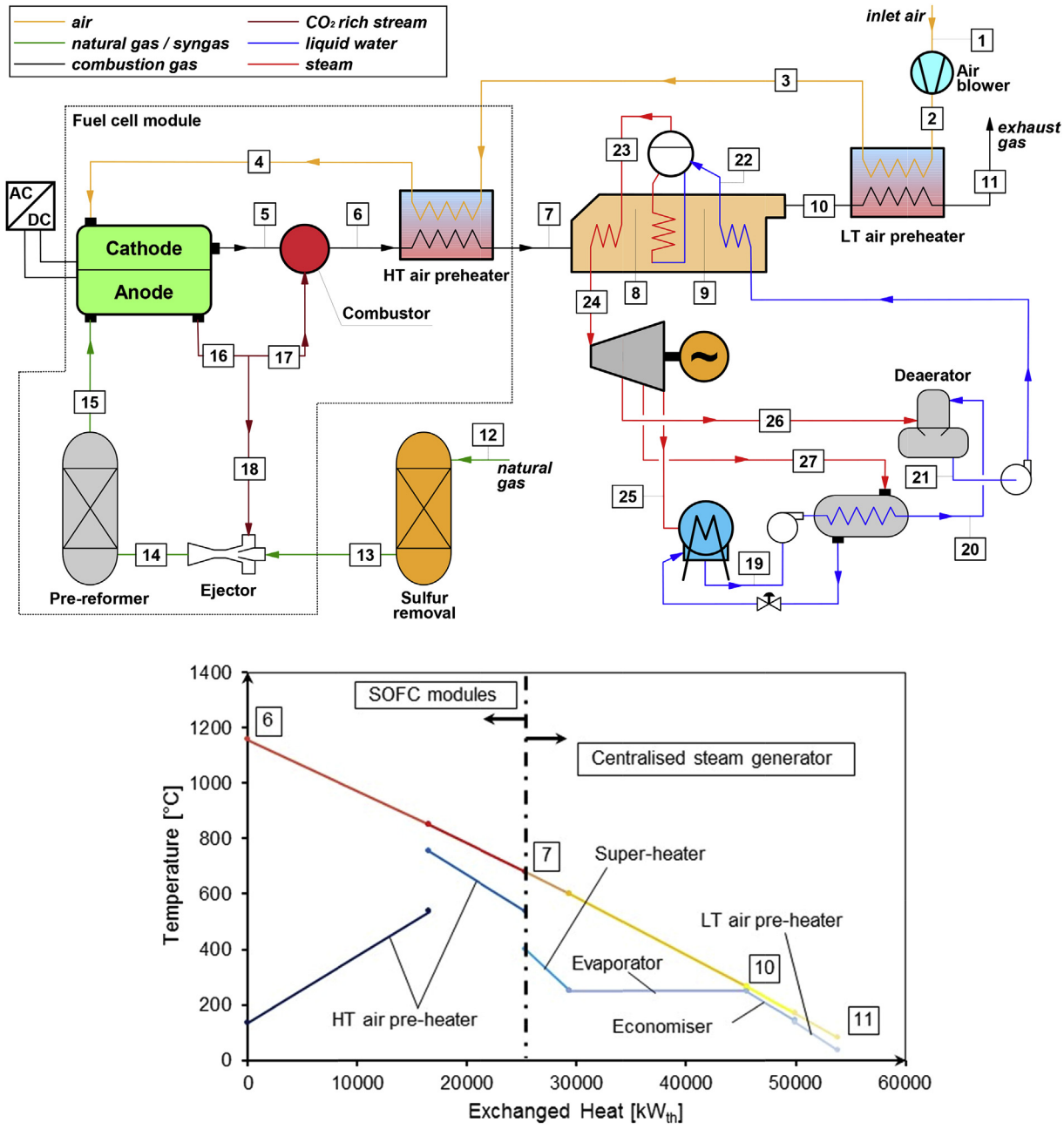

Fig. 5. Atmospheric SOFC + ST power plant without CCS (above) and related cumulative Temperature-Heat duty diagram (below) for the SOFC module exhaust gases cooling section.

the adoption of adequate flow distribution geometries; indeed such voltage could not be obtained with a simple co-flow arrangement, due to limitations on the Nernst voltage at cell outlet. On the other hand, counter-flow geometries as well as multiple-pass or flow splitting arrangements allow increasing the reactant utilization without penalizing the voltage, as discussed by Li et al. for the analysis of IGFC cycles [73] and introduced by Selimovic [74], while avoiding hot spots and too steep thermal gradients within the cell. Discussion of flow arrangement effects on SOFC performance requires 1D or multi-dimensional model-ling approaches [44,73], which will be applied in future work related to this analysis.

The bottoming cycle turns out to be a medium-scale steam cy-cle; its thermodynamic conditions and plant configuration are consistent with those reported by Consonni et al. [70] for similar size waste-to-energy Rankine cycles. The turbine isentropic efficiency has been assumed at 85%, reflecting an optimized design [63].

In this layout, the most critical operating conditions are found in the high temperature air pre-heater. In order to limit the heat exchanger wall temperature, proper arrangement of the streams should be considered. For example, the HT air preheater may be arranged with the hottest section with co-current flow configuration and the colder section with counter-current flows, allowing to achieve the target air temperature while keeping sufficiently low wall temperatures. This configuration is considered in the lower part of Fig. 5, showing the temperature – heat duty diagram of the heat exchanger network. The details about stream

Table 3
Simulation assumptions.

Ambient conditions	
Temperature [°C]	15.0
Pressure [bar]	1.013
Relative humidity [%]	60.0
Natural gas chemical properties	
Molar composition [%mol]	CH_4: 89.0, CO_2: 2.0, C_2H_6: 7.0, C_3H_8: 1.0, N_2: 0.89, C_4H_{10}: 0.11
LHV [MJ/kg]	46.482
Fuel LHV power input [MW_{th}]	100.0
SOFC	
Minimum air inlet temperature [°C]	735.0
Anode and cathode outlet temperature [°C]	800.0
Cell voltage [V]	0.86
Fuel utilization factor (overall) [%]	85.0
Minimum O_2 molar fraction at SOFC outlet [%mol]	5.0
Air and fuel channels pressure losses [%]	3.0
Heat loss [% of fuel LHV]	2.0
DC/AC electrical efficiency [%]	97.0
Inter-cooled recuperative gas turbine (IC-RGT)	
Inlet air filter pressure loss [%]	1.0
LP compressor pressure ratio [−]	2.068
HP compressor pressure ratio [−]	2.0
HP/LP compressors polytropic efficiency [%]	89.7/88.9
Combustor pressure losses [%]	3.0
Turbine polytropic efficiency [%]	92.3
Mechanical efficiency of compressor/turbine [%]	99.7
Generator electric efficiency [%]	98.0
Maximum TIT [°C]	950.0
GT rotating speed [rpm]	8000
Steam cycle	
Evaporation pressure [bar]	40.0
Maximum steam temperature [°C]	400.0
Subcooling ΔT at evaporator drum inlet [°C]	5.0
Pressure drop at steam turbine inlet [%]	5.0
Pressure drop in steam super-heater	3.5
Pressure drop in evaporator [%]	0.0
Pressure drop in economiser [%]	20.0
Temperature drop in superheater to turbine piping [°C]	2.0
Condensing pressure [bar]	0.048
Turbine isentropic efficiency [%]	85.0 [63]
Feed water pump hydraulic efficiency [%]	85.0
Turbine mechanical efficiency [%]	99.6
Generator electric efficiency [%]	98.5
Pre-reformer	
Pre-reformer inlet S/C ratio[a] [−]	2.0
Low temperature sulphur removal	
Operating temperature [°C]	15.0
Fuel pressure loss $\Delta p/p_{in}$ [%]	3.0
Heat exchangers	
Hot and cold side $\Delta p/p_{in}$ [%]	2.0
LT and HT air regenerators $\Delta p/p_{in}$ [%]	3.0
Heat losses [% of heat transferred]	0.7
Minimum gas-evaporating water ΔT (pinch-point) [°C]	10
Minimum ΔT in gas—water heat exchangers [°C]	15
Minimum ΔT in gas—gas heat exchangers [°C]	30
Miscellaneous	
Minimum combustor outlet O_2 molar fraction [%mol]	1.5
Minimum exhaust temperature at stack [°C]	80.0
Air fan isentropic efficiency [%]	80.0
Air fan mechanical-electrical efficiency [%]	94.0
Electric auxiliaries for heat rejection [% of heat rejected]	0.8

[a] S/C value has been calculated vs. reactive carbon-based molecules (i.e. total carbon except CO_2).

thermodynamic conditions and chemical compositions are reported in Table 4.

Based on SOFC performance discussed at point 2.2 and optimizing the bottoming cycle parameters, it is possible to achieve a very high overall cycle electrical efficiency, exceeding 75% LHV, as reported in the following.

4.2. Pressurized SOFC + GT cycle

The proposed power cycle is an evolution of the cycle originally described in Campanari and Chiesa [25,26]. Original results were very attractive in terms of thermodynamic balances, reaching a 69.3% net electric efficiency with 90% CO_2 capture, using an intercooled gas turbine cycle (pressure ratio close to 4, turbine inlet temperature 900 °C), without bottoming cycles. The estimated cycle efficiency without CO_2 capture was about 72%. The original configuration of this power cycle was based on fuel cells operating at around 1000 °C, corresponding to first-generation SOFCs developed in the '90s and early 2000. Assuming the cell voltage at 0.7 V, the SOFC delivered about 74% of the total power output, the remaining being generated by the syngas expander and the gas turbine. Thanks to the high SOFC temperature, the GT cycle operated with a turbine inlet temperature close to 900 °C, allowing to obtain a significant power production from the gas turbine cycle.

The configuration we propose in this work is an evolution of that power cycle layout, considering the SOFC performance discussed in Section 3.2. As shown in Fig. 6, it differs from the original one in several points:

- The SOFC works with a very high fraction of internal reforming, since the low temperature pre-reformer (the equilibrium temperature is 568.1 °C) acts mainly on higher hydrocarbons (i.e. C_2H_6, C_3H_8, C_4H_{10} in our simulations) which are reformed before entering the fuel cell;
- The lower SOFC operating temperature brings about a redesign of the heat recovery and air preheating section, now exploiting high temperature thermal power from anode exhaust cooling and lower quality heat to pre-heat air in the recuperative heat exchanger of the gas turbine engine.
- Steam injection in the gas turbine is no longer adopted, aiming to avoid any external supply of demineralized water.

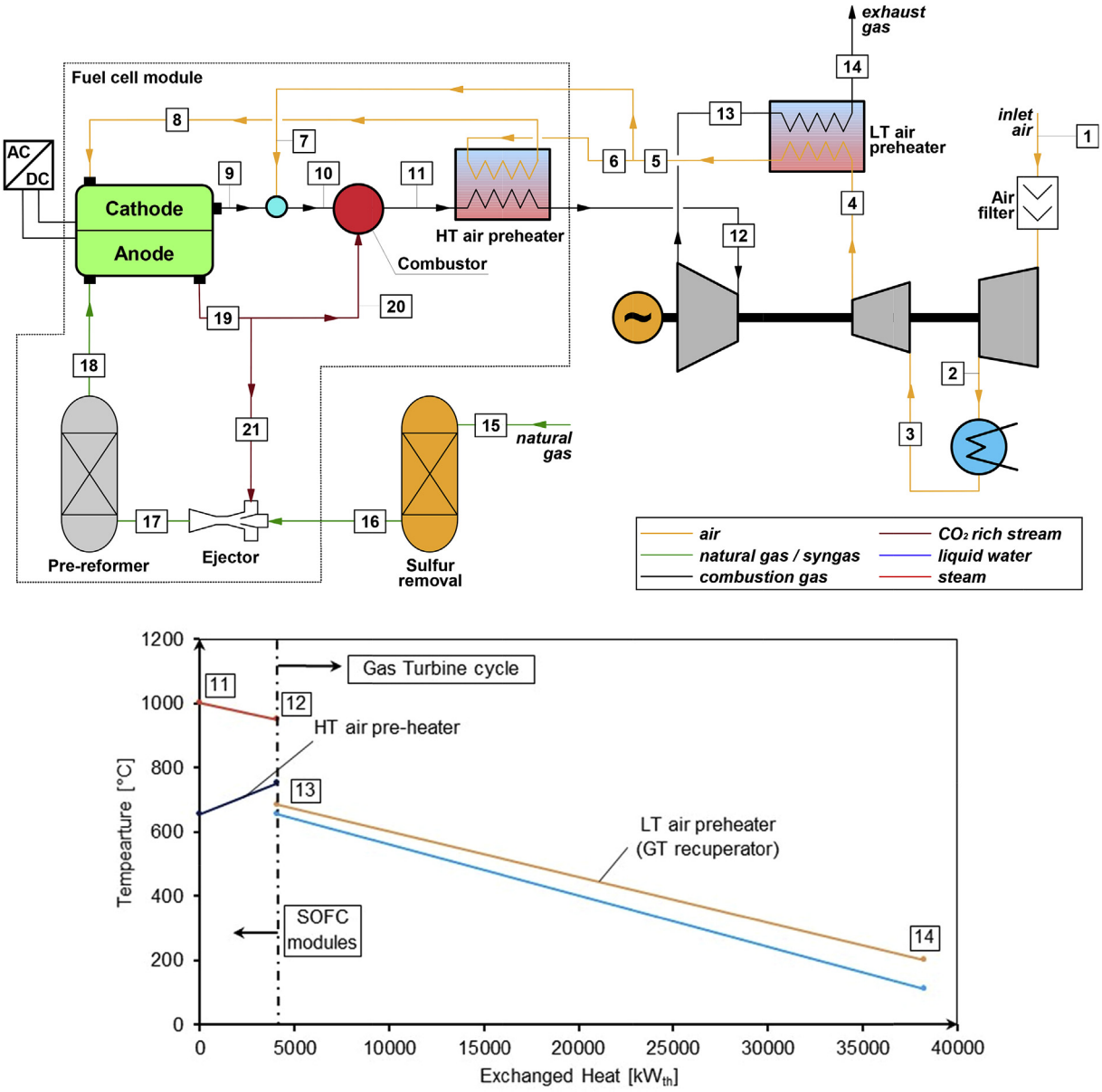

Fig. 6. Pressurized SOFC + GT power plant without CO_2 capture (above) and related cumulative Temperature-Heat duty diagram (below) of the air heating section.

Table 4
Thermodynamic conditions and chemical compositions of the main streams of atmospheric SOFC + ST power plant without CO_2 capture.

Stream	T [°C]	P [bar]	G [mol s^{-1}]	M [kg s^{-1}]	m × LHV	Composition [%mol]								
					[MW]	Ar	CH_4	CO	CO_2	C+	H_2	H_2O	N_2	O_2
1	15.0	1.00	1302.20	37.6	–	0.92	–	–	0.03	–	–	1.03	77.28	20.73
2	34.3	1.20	1302.20	37.6	–	0.92	–	–	0.03	–	–	1.03	77.28	20.73
3	131.0	1.19	1302.20	37.6	–	0.92	–	–	0.03	–	–	1.03	77.28	20.73
4	753.8	1.16	1302.20	37.6	–	0.92	–	–	0.03	–	–	1.03	77.28	20.73
5	799.9	1.12	1090.80	30.8	–	1.10	–	–	0.04	–	–	1.24	92.26	5.37
6	1155.8	1.09	1427.20	39.7	–	0.84	–	–	9.10	–	–	17.98	70.59	1.50
7	679.1	1.05	1427.20	39.7	–	0.84	–	–	9.10	–	–	17.98	70.59	1.50
8	600.3	1.04	1427.20	39.7	–	0.84	–	–	9.10	–	–	17.98	70.59	1.50
9	263.5	1.04	1427.20	39.7	–	0.84	–	–	9.10	–	–	17.98	70.59	1.50
10	166.8	1.02	1427.20	39.7	–	0.84	–	–	9.10	–	–	17.98	70.59	1.50
11	80.0	1.01	1427.20	39.7	–	0.84	–	–	9.10	–	–	17.98	70.59	1.50
12	15.0	20.00	119.40	2.2	100.0	–	89.00	–	2.00	8.11	–	–	0.89	–
13	15.0	19.40	119.40	2.2	100.0	–	89.00	–	2.00	8.11	–	–	0.89	–
14	651.9	1.20	781.09	17.9	133.5	–	13.61	5.07	24.59	1.24	11.81	43.30	0.38	–
15	520.6	1.16	841.04	17.9	137.7	–	11.55	4.45	26.66	–	24.16	32.83	0.35	–
16	799.9	1.13	1035.30	24.7	52.5	–	–	5.99	28.67	–	13.94	51.11	0.28	–
17	799.9	1.13	373.59	8.9	18.9	–	–	5.99	28.67	–	13.94	51.11	0.28	–
18	799.9	1.13	661.68	15.8	33.5	–	–	5.99	28.67	–	13.94	51.11	0.28	–
19	32.3	0.048	482.92	8.7	–	–	–	–	–	–	–	100	–	–
20	104.1	5.60	483.48	8.7	–	–	–	–	–	–	–	100	–	–
21	139.9	3.60	517.34	9.3	–	–	–	–	–	–	–	100	–	–
22	245.4	40.00	517.12	9.3	–	–	–	–	–	–	–	100	–	–
23	250.4	40.00	517.12	9.3	–	–	–	–	–	–	–	100	–	–
24	398.0	36.67	517.12	9.3	–	–	–	–	–	–	–	100	–	–
25	32.2	0.048	403.05	7.3	–	–	–	–	–	–	–	100	–	–
26	148.7	3.79	34.14	0.6	–	–	–	–	–	–	–	100	–	–
27	108.6	1.37	60.00	1.1	–	–	–	–	–	–	–	100	–	–

With respect to the SOFC + ST case, the HT air preheaters located close to the SOFC modules feature a much lower overall thermal duty (~4.0 vs. 25.5 MW_{th}) and lower, although still demanding, expected wall temperatures due to the lower temperature of the gas from the combustor. Aiming to reduce the maximum wall temperatures, the HT air preheater work in a co-current configuration. As a partial counterpart, the cycle adopts a large centralized gas-air recuperator in the GT cycle, featuring a thermal duty of about 38 MW_{th}. The temperature-heat diagram of this plant is shown in the lower part of Fig. 6.

The air mass flow rate at compressor inlet is about 58.1 kg s^{-1}, similar to a mid-size aero-derivative gas turbine; however, given the low TIT, necessary to avoid the use of blade cooling, the power output of the gas turbine cycle is limited to 10.7 MW, with an electric specific work of 184 kJ kg^{-1} (vs. typical values of 350–450 kJ kg^{-1} for state-of-the-art gas turbines). To recover the flue gas heat at the recuperator outlet and given that no bottoming cycles (e.g. organic Rankine cycles-ORC) are used, an intercooled GT configuration has been chosen despite the limited pressure ratio. As a matter of fact, an additional bottoming cycle would have introduced additional plant complications without giving a remarkable performance benefit; on the other hand, the

Table 5
Thermodynamic conditions and chemical compositions of the main streams of pressurized SOFC + GT power plant without CCS.

Stream	T [°C]	P [bar]	G [mol s^{-1}]	M [kg s^{-1}]	m × LHV	Composition [%mol]								
					[MW]	Ar	CH_4	CO	CO_2	C+	H_2	H_2O	N_2	O_2
1	15.0	1.01	2015.40	58.1	–	0.92	–	–	0.03	–	–	1.03	77.28	20.73
2	89.5	2.07	2015.40	58.1	–	0.92	–	–	0.03	–	–	1.03	77.28	20.73
3	35.0	2.03	2015.40	58.1	–	0.92	–	–	0.03	–	–	1.03	77.28	20.73
4	111.1	4.07	2015.40	58.1	–	0.92	–	–	0.03	–	–	1.03	77.28	20.73
5	656.0	4.07	2015.40	58.1	–	0.92	–	–	0.03	–	–	1.03	77.28	20.73
6	656.0	4.07	1278.60	36.9	–	0.92	–	–	0.03	–	–	1.03	77.28	20.73
7	656.0	4.07	736.79	21.3	–	0.92	–	–	0.03	–	–	1.03	77.28	20.73
8	752.2	3.83	1278.60	36.9	–	0.92	–	–	0.03	–	–	1.03	77.28	20.73
9	799.9	3.72	1067.30	30.1	–	1.10	–	–	0.04	–	–	1.24	92.59	5.03
10	741.2	3.72	1804.10	51.4	–	1.03	–	–	0.03	–	–	1.16	86.34	11.45
11	1002.1	3.60	2140.40	60.3	–	0.87	–	–	6.08	–	–	12.33	72.82	7.91
12	949.9	3.51	2140.40	60.3	–	0.87	–	–	6.08	–	–	12.33	72.82	7.91
13	686.0	1.03	2140.40	60.3	–	0.87	–	–	6.08	–	–	12.33	72.82	7.91
14	200.9	1.01	2140.40	60.3	–	0.87	–	–	6.08	–	–	12.33	72.82	7.91
15	15.0	20.00	119.41	2.2	100.0	–	89.00	–	2.00	8.11	–	–	0.89	–
16	15.0	19.40	119.41	2.2	100.0	–	89.00	–	2.00	8.11	–	–	0.89	–
17	651.9	4.41	781.10	17.9	133.5	–	13.61	5.07	24.59	1.24	11.81	43.30	0.38	–
18	568.1	4.28	822.78	17.9	136.2	–	12.92	4.58	26.12	–	20.23	35.81	0.36	–
19	799.9	4.15	1035.30	24.7	52.5	–	–	5.99	28.67	–	13.94	51.11	0.28	–
20	799.9	4.15	373.60	8.9	18.9	–	–	5.99	28.67	–	13.94	51.11	0.28	–
21	799.9	4.15	661.70	15.8	33.5	–	–	5.99	28.67	–	13.94	51.11	0.28	–

Table 6
Overall energy balances of pressurized (SOFC + GT) and atmospheric (SOFC + ST) power plants, without CCS.

Plant performance	Atmospheric plant (SOFC + ST)	Pressurized plant (SOFC + GT)
Fuel inlet (LHV) [MW]	100	100
Fuel cell net AC power [MW]	68.06	68.06
GT net electric power [MW]	–	10.71
ST electric power [MW]	8.06	–
Auxiliaries electric power [MW]	−0.91	−0.03
Net electric power [MW]	75.20	78.74
Net electric efficiency HHV [%]	67.93	71.14
Net electric efficiency LHV [%]	75.20	78.74
CO_2 emission [kg s^{-1}]	5.72	5.72
CO_2 specific emission [kg MWh^{-1}]	273.59	260.50

chosen design reduces the GT compressor consumption, thus increasing the gas turbine specific work output, although adding the costs related to the intercooler.

As already discussed for the atmospheric plant, the air utilization is set to achieve a cell outlet temperature of 800 °C, here reaching 79.7% (the specific work generated by the cell is 1900.3 kJ kg_{air}^{-1} and 3918 kJ kg_{fuel}^{-1}). This allows also keeping a sufficiently high turbine inlet temperature and decreasing the required air mass flow rate handled by the gas turbine cycle.

It can be noted from Fig. 6 that the arrangement of the SOFC module remains unchanged compared to the atmospheric reference case; the only modification in the plant layout is the presence of a by-pass air stream (point #7) required to comply with the limitations on the maximum turbine inlet temperature. A minor difference comes from the different equilibrium of the pre-reforming reaction, moving towards the reactants due to pressurization, thus leading to a larger reforming effect within the fuel cell channels and lower cooling air requirement.

The cell voltage has been kept for simplicity to the value of 0.86 V, resulting from the reference SOFC calibration, neglecting both the positive effects on the current density due to pressuri-zation and the negative effects of the higher air utilization factor and the increased electronic leakage current, which generally characterises the high pressure operation [38]. However, a sensi-tivity analysis is reported in Part B of this work to highlight the effects of different fuel cell operating voltages and fuel utilization on plant performance. The final results are significantly different from the original papers [25,26], but confirm the possibility of reaching very high overall efficiencies. Details about composition and thermodynamic properties of most relevant streams are shown in Table 5.

5. Comparison of the power cycles

The power balance of the two plants assessed is shown in Table 6 and is sustained in both cases primarily by the SOFC, which generates 86.4% and 90.5% of the net power output, respectively in the pressurized and in the atmospheric case. The gas turbine and steam power cycles account for the production of the complementary power generation. Both power cycles reach an extremely high net electrical efficiency, 3.5% higher for the pressurized plant (78.74% vs. 75.20%). From a first law analysis, the reported difference in terms of attained overall efficiencies is mainly related to the nature and the amount of energy dissipated to the environment; the condenser is the main component for low temperature energy dissipation in the SOFC + ST configuration and accounts for 16.0% of efficiency penalty; in addition, the stack losses constitute the sec-ond most important dissipation term, 8.73% of the total inlet thermal power. Comparing the two losses in the atmospheric and in the pressurized cases, the SOFC + GT results in a lower energy dissipation (21.3% vs. 24.7%).

5.1. Second-law analysis

A better thermodynamic understanding of the results can be obtained by means of a second law analysis. The second law efficiency is defined as [60]:

$$\eta_{II} = \frac{P_{el}}{Ex_f \times m_f} \tag{6}$$

while the second law losses are defined as:

Table 7
Second law analysis of the considered cycles.

II law losses $\Delta\eta_{II}$ (%)	Cycle configuration	
	Atmospheric SOFC + ST	Pressurized SOFC + GT
I. SOFC Electrochemical Reactions	3.600	3.470
II. Other SOFC losses	3.354	3.355
III. Combustor	4.160	5.141
IV. Air blower/compressor	0.135	0.744
V. Turbine	–	0.866
VI. Mech., el. and auxiliary	0.045	0.552
VII. GT Recuperator	–	1.796
VIII. Air HT pre-heater	4.667	0.568
IX. HRSG	3.057	–
X. Other heat and pressure losses	2.791	2.649
XI. Stack/Waste heat losses	3.297	6.333
XII. Pre-reformer	0.448	0.293
XIII. Steam cycle	2.685	–
Second law efficiency η_{II}	71.761	74.233
Inlet fuel exergy [MW]	104.97	104.97

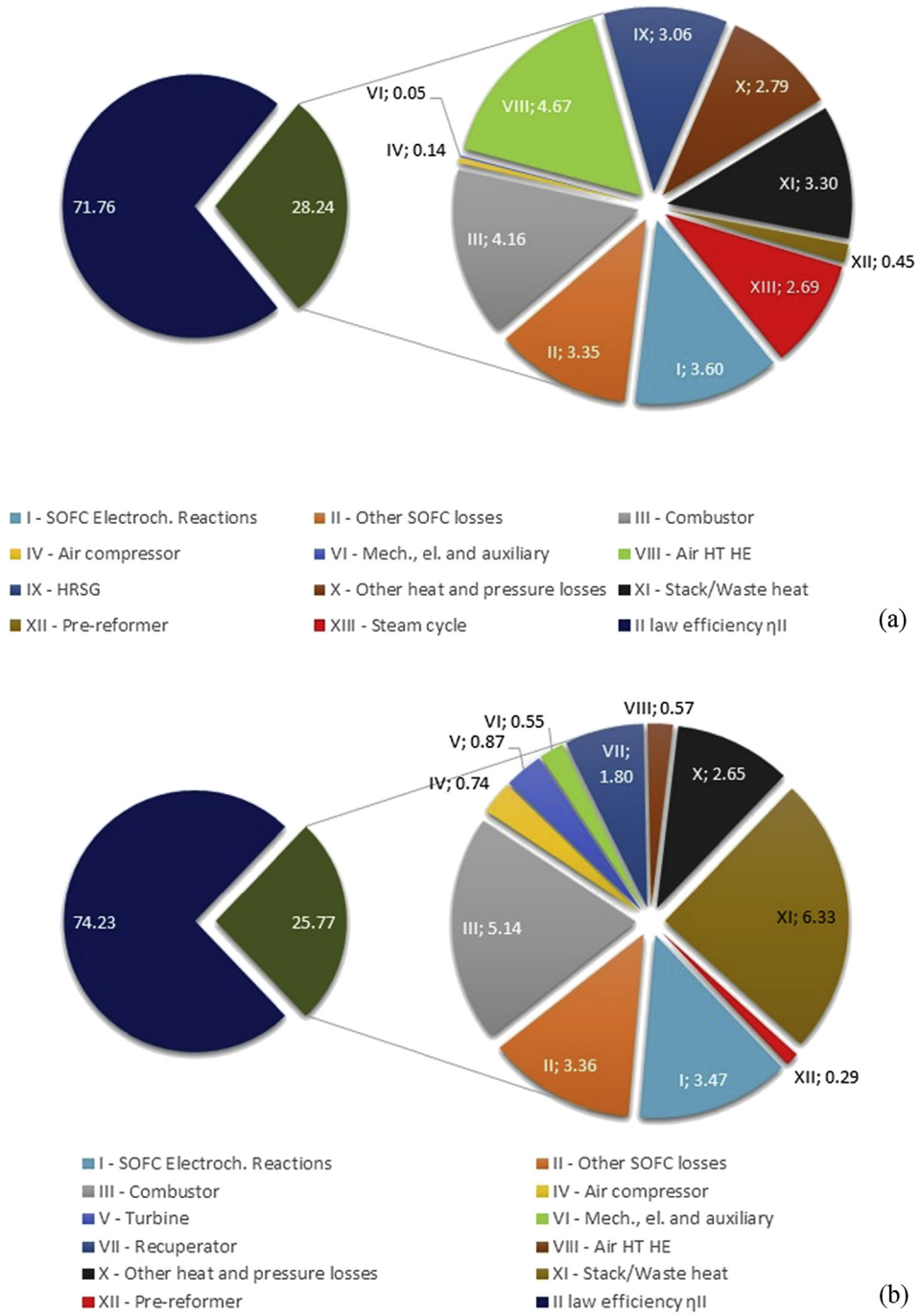

Fig. 7. Irreversibility repartition in the a) SOFC + ST and b) SOFC + GT power plant configurations.

$$\Delta\eta_{II} = \frac{T_{amb}\Delta S}{Ex_f \times m_f} \tag{7}$$

Table 7 gives the various second-law efficiency losses, grouped in the following terms:

I Irreversibility occurring in the fuel cell for electrochemical reactions and internal heat Exchange
II $\Delta\eta_{II}$ other irreversibility losses occurring in the fuel cell (including power conditioning, heat losses, pressure drops, etc.)
III Irreversibility of the combustion
IV Fluid-dynamic losses for air compression
V Turbine expansion fluid-dynamic losses
VI $\Delta\eta_{II}$ all GT mechanical/electrical losses and cycle auxiliary losses
VII Heat transfer, heat losses and pressure drops occurring in the gas turbine recuperator
VIII Heat transfer, heat losses and pressure drops occurring in the HT air pre-heater
IX Heat transfer, heat losses and pressure drops occurring in the HRSG

X Heat transfer, heat losses and pressure drops occurring in all other heat exchangers, filters, ducting and valves
XI Stack/waste heat losses
XII Irreversibility of the pre-reformer reaction
XIII Irreversibility of the steam cycle

Results are expressed graphically in Fig. 7. The second law analysis suggests that:

- The atmospheric case is characterised by larger thermal and heat transfer losses compared to the pressurized plant. This is mainly due to high irreversibility in the HT air pre-heater (4.667%), which features rather large temperature differences and an important heat duty (25 MW, see Fig. 7), in the HRSG (2.95%) and the additional losses of various nature related to the steam cycle.
- The pressurized case, on the other hand, requires a recuperator which brings about lower irreversible losses (1.80%) thanks to the smaller temperature differences, although featuring a larger heat duty (34.2 MW, see Fig. 6).
- As expected, stack losses in the pressurized SOFC + GT configuration are higher than in the SOFC + ST but less detrimental in the second law balances compared to their efficiency penalties computed with the energy balance. On the other hand, the second law analysis shows that the main exergy dissipations are associated to the combustion and the electrochemical oxidation processes. In both proposed cycles the electrochemical losses and the combustor losses are comparable in magnitude (11.11% and 11.96%). On the whole, the greater thermodynamic efficiency of the electrochemical devices compared to conventional fuel oxidation processes is confirmed.
- The total value of SOFC losses is limited and ranges between 6.8% and 7.0%, indicating that further SOFC performance improvements would impact on rather small figures. It is noteworthy that the losses due to the pure electrochemical oxidation process result comparable to those of the other SOFC processes (heat and pressure losses, DC/AC conversion).

6. Conclusions

This work presented the thermodynamic analysis of two ultra-high efficiency SOFC power cycles designed for electricity generation using natural gas as a fuel. In this Part A of the work, only cases without CO_2 capture were considered. With the aim of having a well-defined simulation framework, particular attention was dedicated to highlight the operating conditions and the assumptions adopted for each plant component. Following a comprehensive analysis of possible plant configurations with respect to the main design options, the proposed plants are based on an integrated-reforming concept where fuel is reformed within the SOFC, operated at intermediate temperature (about 750 °C). The fuel cell follows the specifications of a state-of-the-art advanced unit, representative of 60% + electrical efficiency SOFCs. Concerning the two plant configurations, the first considers a FC working at atmospheric pressure, whereas the second is based on a moderately pressurized stack (named SOFC + SC and SOFC + GT, respectively). Accordingly, the excess heat in the cell exhaust is recovered with a Rankine cycle in the former and with a Brayton cycle in the latter.

Results show that both the configurations feature a very high net electrical efficiency: 75.20% and 78.74% (LHV basis) for SOFC + SC and SOFC + GT, respectively. While on one hand the SOFC + GT plant shows a higher efficiency, on the other it requires a pressurized stack system. With the aim of identifying the major contributions to the degradation from chemical to thermal energy, the proposed solutions were also investigated from a second-law perspective. The second law efficiencies confirmed the quality of the electrochemical processes: overall SOFC losses are limited to 6.8–7.0% despite being the primary power output source. Including combustion of anode exhaust, the irreversibility for fuel oxidation globally accounts for about 12% of the input exergy. Considered that fuel combustion in an advanced gas turbine of a state-of-the-art combined cycle entails an efficiency loss which is almost twice larger, it is clear the reason of the efficiency advantage compared to combined cycles.

Acknowledgements

The authors wish to thanks Edison SpA for partly supporting the work related to this study.

References

[1] IPCC Climate Change 2013: the Physical Science Basis, Cambridge University Press, 2014.
[2] J.H. Hirschenhofer, D.B. Staffer, J.S. White, Carbon Dioxide Capture in Fuel Cell Power Systems, International Energy Conversion Engineering Conference, New York, 1994.
[3] EG&G Technical Services Fuel Cell Handbook, seventh ed., U.S. Department of Energy, 2004.
[4] D. Carter, J. Wing, The Fuel Cell Today Industry Review 2013, Sept. 2013. www.fuelcelltoday.com.
[5] D. Rastler, Program on Technology Innovation: Systems Assessment of Direct Carbon Fuel Cells Technology Electric Power Research Institute (EPRI), 2008. Report No. 1016170.
[6] S. Campanari, M. Gazzani, M.C. Romano, Analysis of direct carbon fuel cell (DCFC) based coal fired power cycles with CO2 capture, J. Eng. Gas Turbines Power 135 (1) (2013), http://dx.doi.org/10.1115/1.4007354.
[7] S. Ghosh, S. De, Thermodynamic performance study of an integrated gasification fuel cell combined cycle—an energy analysis, Proc. Inst. Mech. Eng. Part A 217 (2003) 137–147.
[8] T. Kivisaari, P. Björnbom, C. Sylwan, B. Jacquinot, D. Jansen, A. de Groot, The feasibility of a coal gasifier combined with a high-temperature fuel cell, Chem. Eng. J. 100 (1–3) (2004) 167–180.
[9] M.C. Romano, S. Campanari, V. Spallina, G. Lozza, Thermodynamic analysis and optimization of IT-SOFC-based integrated coal gasification fuel cell power plants, J. Fuel Cell Sci. Technol. 8 (4) (2011).
[10] A. Verma, A.D. Rao, G.S. Samuelsen, Sensitivity analysis of a,Vision 21 coal based zero emission power plant, J. Power Sour. 158 (1) (2006) 417–427.
[11] V. Spallina, M.C. Romano, S. Campanari, G. Lozza, A SOFC-based integrated gasification fuel cell cycle with CO_2 capture, J. Eng. Gas Turbines Power 133 (7) (2011) 071706.
[12] A. Lanzini, T.G. Kreutz, E. Martelli, M. Santarelli, Energy and economic performance of novel integrated gasifier fuel cell (IGFC) cycles with carbon capture, Int. J. Greenh. Gas Control 26 (2014) 169–184.
[13] M. Li, A.D. Rao, J. Brouwer, G.S. Samuelsen, Design of highly efficient coal-based integrated gasification fuel cell power plants, J. Power Sour. 195 (2010) 5707–5718.
[14] S. Veyo, et al., Tubular solid oxide fuel cell/gas turbine hybrid cycle power systems – status, in: ASME Turbo Expo 2000-GT-550, 2000.
[15] S. Campanari, E. Macchi, Thermodynamic analysis of advanced power cycles based upon solid oxide fuel cells, gas turbines and Rankine bottoming cycles, in: Proc. of ASME Turbo Expo, 98-GT-585, Stockholm, 1998.
[16] M. Rokni, Thermodynamic analysis of an integrated solid oxide fuel cell cycle with a Rankine cycle, Energy Convers. Manag. 51 (12) (Dec. 2010) 2724–2732.
[17] http://www.fuelcellenergy.com/, 2015.
[18] K. Foger, T. Rowe, Ultra-high-efficiency residential power system, in: 3rd European Fuel Cell Technology Applications Conference, Rome, Dec. 2009.
[19] http://www.cfcl.com.au, 2015.
[20] H. Ghezel-Ayagh, Advances in SOFC development at fuelcell energy, in: 14th Annual SECA Workshop, Pittsburgh, PA, July 23-24, 2013.
[21] http://www.solidpower.com, 2015.
[22] L. Mastropasqua, S. Campanari, P. Iora, M.C. Romano, Simulation of intermediate-temperature SOFC for 60%+ efficiency distributed generation, in: Proc. of ASME 2015 Power and Energy Conversion Conference, Power-Energy 2015–49373, USA, June 2015.
[23] A. Hussain, Meeting energy needs – comparing the electricity options: Bloom Energy vision, in: Plenary Session Presentation at ASME 2015 Power and Energy Conversion Conference, USA, June 2015.
[24] http://www.bloomenergy.com, 2015.
[25] S. Campanari, P. Chiesa, Potential of solid oxide fuel cells (SOFC) based cycles in low-CO_2 emission power generation, in: Proc. Fifth International Conference on Greenhouse Gas Control Technologies, GHGT-5, Cairns, Australia, 2000.

[26] S. Campanari, Carbon dioxide separation from high temperature fuel cell power plants, J. Power Sour. 112 (2002) 273–289.

[27] M. Akai, N. Nomuna, H. Waku, M. Inoue, Life-cycle analysis of a fossil-fuel power plant with CO_2 recovery and a sequestering system, Energy 22 (1997) 249–255.

[28] T.A. Adams, J. Nease, D.P. Tucker, Energy conversion with solid oxide fuel cell systems: a review of concepts and outlooks for the short- and long-term, Ind. Eng. Chem. Res. 52 (2013) 3089–3111.

[29] T.A. Adams, P.I. Barton, High-efficiency power production from natural gas with carbon capture, J. Power Sour. 195 (2010) 1971–1983.

[30] B.F. Moller, J. Arriagada, M. Assadi, I. Potts, Optimisation of an SOFC/GT system with CO_2-capture, J. Power Sour. 131 (2004) 320–326.

[31] S. Campanari, M. Gazzani, High efficiency SOFC power cycles with indirect natural gas reforming and CO_2 capture, J. Fuel Cell Sci. Technol. 12 (2) (2015), http://dx.doi.org/10.1115/1.4029425.

[32] L. Duan, Y. Yang, B. He, G. Xu, Study on a novel solid oxide fuel cell/gas turbine hybrid cycle system with CO2 capture, Int. J. Energy Res. 36 (2012) 139–152.

[33] E. Macchi, S. Campanari, P. Silva, Natural Gas Micro-cogeneration and Thermally-driven HVAC Systems, Polipress, Milano, 2012, p. 368 (in Italian) ISBN 97888-7398-073-5.

[34] K.P. Litzinger, S.E. Veyo, L.A. Shockling, W.L. Lundberg, Comparative evaluation of SOFC/gas turbine hybrid system options, in: Proc. of ASME Turbo Expo, GT2005–68909, Reno-Tahoe, NV, USA, June 2005.

[35] S. Campanari, Parametric analysis of small scale recuperated SOFC/gas turbine cycles, in: ASME Turbo Expo 2004-GT-53933, 2004.

[36] S.J. McPhail, L. Leto, C. Boigues-Muñoz, The yellow pages of SOFC technology – International status of SOFC deployment 2012-2013. IEA Implementing Agreement Advanced Fuel Cells Annex 24, ENEA, 2013. ISBN 978-88-8286-290-9.

[37] W.C. Chueh, Y. Hao, W. Jung, S.M. Haile, High electrochemical activity of the oxide phase in model ceria-Pt and ceria-Ni composite anodes, Nat. Mater. 11 (2) (2012) 155–161.

[38] K. Huang, G.B. John, Solid Oxide Fuel Cell Technology – Principles, Performance and Operations, Woodhead Publishing, 2009.

[39] K. Damen, M. Van Troost, A. Faaij, W. Turkenburg, A comparison of electricity and hydrogen production systems with CO_2 capture and storage. Part A: review and selection of promising conversion and capture technologies, Prog. Energy Combust. Sci. 32 (2006) 215–246.

[40] P. Piroonlerkgul, N. Laosiripojana, A.A. Adesina, S. Assabumrungrat, Performance of biogas-fed solid oxide fuel cell systems integrated with membrane module for CO2 removal, Chem Eng Process 48 (2009) 672–682.

[41] E. Liese, Comparison of pre-anode and post-anode carbon dioxide separation for IGFC systems, in: Proc. of ASME Turbo Expo, GT2009-59144, Orlando, USA, 2009.

[42] M. Powell, K. Meinhardt, V. Sprenkle, L. Chick, G. McVay, Demonstration of a highly efficient solid oxide fuel cell power system using adiabatic steam reforming and anode gas recirculation, J. Power Sour. 205 (2012) 377–384, http://dx.doi.org/10.1016/j.jpowsour.2012.01.098.

[43] P. Aguiar, C.S. Adjiman, N.P. Brandon, Anode-supported intermediate temperature direct internal reforming solid oxide fuel cell. I: model-based steady-state performance, J. Power Sour. 138 (2004) 120–136.

[44] S. Campanari, P. Iora, Comparison of finite volume SOFC models for the simulation of a planar cell geometry, Fuel Cells 5 (2005) 34–51.

[45] H. Iwai, Y. Yamamoto, M. Saito, H. Yoshida, Numerical simulation of intermediate-temperature direct-internal-reforming planar solid oxide fuel cell, Energy 36 (2011) 2225–2234.

[46] J.W. Dijkstra, D. Jansen, Novel concepts for CO_2 capture, Energy 29 (2004) 1249–1257.

[47] M.L. Ferrari, M. Pascenti, A.F. Massardo, Ejector model for high temperature fuel cell hybrid systems: experimental validation at steady-state and dynamic conditions, J. Fuel Cell Sci. Technol. 5 (4) (2008) 041005.

[48] H. Jericha, V. Hacker, W. Sanz, G. Zotter, Thermal steam power plant fired by hydrogen and oxygen in stoichiometric ratio, using fuel cells and gas turbine cycle components, in: Proc. of ASME Turbo Expo, GT2010-22282, Glasgow, UK, 2010.

[49] G.O. Alptekin, A. Jayaraman, M. Dubovik, M. Schaefer, W. Mike, K. Bradley, Natural Gas Desulfurization for Fuel Cell Applications by Adsorption, 2008.

[50] M.C. Romano, V. Spallina, S. Campanari, Integrating IT-SOFC and gasification combined cycle with methanation reactor and hydrogen firing for near zero-emission power generation from coal, Energy Proced. 4 (2011) 1168–1175.

[51] E. Riensche, E. Achenbach, D. Froning, M.R. Haines, W.K. Heidug, A. Lokurlu, S. Von Andrian, Clean combined-cycle SOFC power plant — cell modelling and process analysis, J. Power Sour. 86 (2000) 404–410.

[52] F. Trasino, M. Bozzolo, L. Magistri, A.F. Massardo, Modelling and performance analysis of the Rolls-Royce fuel cell system limited 1 MW plant, in: Proc. of ASME Turbo Expo, GT2009-59328, Orlando, USA, June 2009.

[53] G.D. Agnew, R.R. Moritz, C. Berns, A. Spangler, O. Tarnowski, M. Bozzolo, A unique solution to low cost SOFC hybrid power plant, in: Proc. of ASME Turbo Expo, ASME GT2003-38944, Atlanta, USA, June 2003.

[54] A.D. Rao, A. Verma, G.S. Samuelsen, Engineering and economic analyses of a coal-fueled solid oxide fuel cell hybrid power plant, in: ASME Turbo Expo 2005, GT2005–68762, 2005, http://dx.doi.org/10.1115/GT2005-68762.

[55] S.K. Park, T.S. Kim, J.L. Sohn, Y.D. Lee, An integrated power generation system combining solid oxide fuel cell and oxy-fuel combustion for high performance and CO2 capture, Appl. Energy 88 (2011) 1187–1196.

[56] S. Campanari, P. Chiesa, G. Manzolini, CO_2 capture from combined cycles integrated with molten carbonate fuel cells, Int. J. Greenh. Gas Control 4 (2009) 441–451.

[57] J.L. Carson, Thermodynamics of pressure swing adsorption (PSA) in the recovery of residual hydrogen from SOFC anode gas, in: Proc. of Intersociety Energy Conversation Engineering Conference, 1995, pp. 229–234.

[58] M. Gazzani, D.M. Turi, G. Manzolini, Techno-economic assessment of hydrogen selective membranes for CO_2 capture in integrated gasification combined cycle, Int. J. Greenh. Gas Control 20 (2014) 293–309.

[59] P. Chiesa, S. Campanari, G. Manzolini, CO_2 cryogenic separation from combined cycles integrated with molten carbonate fuel cells, Int. J. Hydrogen Energy 36 (16) (2011) 10355–10365.

[60] A. Bejan, Advanced Engineering Thermodynamics, JohnWiley & Sons, NY, 1988.

[61] NIST, Reference Fluid Thermodynamic and Transport Properties Database (REFPROP): Version 9.1, 2015. http://www.nist.gov/srd/nist23.cfm.

[62] S. Consonni, G. Lozza, E. Macchi, P. Chiesa, P. Bombarda, Gas-turbine-based advanced cycles for power generation part A: calculation model, Int. Gas Turbine Conf. Yokohama III (1991) 201–210.

[63] G. Lozza, Bottoming steam cycles for combined gas steam power plants: a theoretical estimation of steam turbine performance and cycle analysis, in: Proc. 1990 ASME Cogen Turbo, New Orleans, LA, USA, ASME, New York, 1990, pp. 83–92.

[64] P. Chiesa, S. Consonni, T. Kreutz, R. Williams, Co-production of hydrogen, electricity and CO_2 from coal with commercially ready technology. Part A: performance and emissions, Int. J. Hydrogen Energy 30 (7) (2005) 747–767.

[65] S. Campanari, P. Iora, E. Macchi, P. Silva, Thermodynamic analysis of integrated MCFC/gas turbine cycles for multi-MW scale power generation, J. Fuel Cell Sci. Tech. 4 (2007) 308–316.

[66] F. Franco, R. Anantharaman, O. Bolland, N. Booth, E. Dorst, C. Van Ekstrom, Common framework and test cases for transparent and comparable techno-economic evaluations of CO_2 capture technologies – the work of the European Benchmarking Task Force, Energy Proced. 1–8 (2010).

[67] Aspen Plus version 2006.5, Aspen Tech. Inc., Cambridge, USA.

[68] http://www.csiropedia.csiro.au/display/CSIROpedia/Ceramic+Fuel+Cells, 2015.

[69] T. Elmer, M. Worall, S. Wu, S.B. Riffat, Emission and economic performance assessment of a solid oxide fuel cell micro-combined heat and power system in a domestic building, Appl. Therm. Eng. 90 (April 2015) 1082–1089.

[70] S. Consonni, F. Viganò, Waste gasification vs. conventional waste-to-Energy: a comparative evaluation of two commercial technologies, Waste Manag. 32 (4) (Apr. 2012) 653–666.

[71] R. Peters, R. Deja, L. Blum, J. Pennanen, J. Kiviaho, T. Hakala, Analysis of solid oxide fuel cell system concepts with anode recycling, Int. J. Hydrogen Energy 38 (16) (May 2013) 6809–6820.

[72] M. Halinen, O. Thomann, J. Kiviaho, Effect of anode off-gas recycling on reforming of natural gas for solid oxide fuel cell systems, Fuel Cells 12 (5) (Oct. 2012) 754–760.

[73] M. Li, J. Brouwer, A.D. Rao, G.S. Samuelsen, Application of a detailed dimensional solid oxide fuel cell model in integrated gasification fuel cell system design and analysis, J. Power Sour. 196 (2011) 5903–5912, http://dx.doi.org/10.1016/j.jpowsour.2011.02.080.

[74] A. Selimovic, J. Palsson, Networked solid oxide fuel cell stacks combined with a gas turbine cycle, J. Power Sour. 106 (1–2) (2002) 76–82.